Materials Research Express

PAPER

Observation of superficial antiferromagnetism in Co_3O_4 polycrystals

To cite this article: Driele von Dreifus *et al* 2015 *Mater. Res. Express* **2** 116102

Materials Research Express

PAPER

Observation of superficial antiferromagnetism in Co_3O_4 polycrystals

Driele von Dreifus[1,2], **Ernesto Chaves Pereira**[1] **and Adilson Jesus Aparecido de Oliveira**[2]

[1] Departamento de Química, Universidade Federal de São Carlos, CP 676, São Carlos, São Paulo, Brazil
[2] Departamento de Física, Universidade Federal de São Carlos, CP 676, São Carlos, São Paulo, Brazil

E-mail: adilson@df.ufscar.br

Keywords: antiferromagnetic phase transition, spinel, magnetization process

RECEIVED
25 August 2015

REVISED
6 October 2015

ACCEPTED FOR PUBLICATION
12 October 2015

PUBLISHED
3 November 2015

Abstract

We report on a systematic study about the magnetic properties of Co_3O_4 polycrystals with large size distribution (100–1200 nm) and the crystallite size of 68(4) nm on average. An antiferromagnetic transition at $T_N = 32$ K, extensively reported in the literature for Co_3O_4, was observed. Furthermore, another transition at $T_t = 14$ K, which is suppressed for $H \geqslant 35$ kOe, was also identified. An increase in the magnetic susceptibility, as well as irreversibility between zero field cooled and field cooled data below T_t were observed. The non-detection of a coercive field below T_t, and the fact that T_t and T_N are independent from the driven frequencies in ac magnetic measurements as a function of temperature, confirm that both peaks are associated to antiferromagnetic transitions.

1. Introduction

Co_3O_4 is a semiconductor, which is technologically important principally due to its applications in lithium batteries [1], heterogeneous catalysis [2], gas sensors [3] and electrochemical capacitors [4]. This oxide has a spinel structure where Co^{3+} ions occupy the octahedral sites and do not contribute to the magnetic properties ($S = 0$), while Co^{2+} ions ($S = 3/2$), which are also present in this phase, occupy the tetrahedral sites forming an antiferromagnetic arrangement at temperatures below $T_N \sim 30$ K [5, 6].

The magnetic properties of the bulk Co_3O_4 sample is well established in the literature [7, 8], although for particle sizes in the nanometer magnitude there are many papers which claim the formation of a metastable state like superparamagnetism and spin-glass [9, 10], which are related to the increase in the surface area volume ratio.

A large number of studies have reported on the antiferromagnetic behavior of Co_3O_4 nanoparticles [11, 12]. Takada *et al* [13] observed that 3 nm Co_3O_4 nanoparticles dispersed in SiO_2 present superparamagnetic behavior with a blocking temperature of $T_B = 3.4$ K. For particles with 15–20 nm, Dutta *et al* [14] observed an antiferromagnetic transition at 35 K, while for bulk samples the transition was observed at 38 K. Furthermore, the authors [14] noted a bifurcation at 29 K between zero field cooled (ZFC) and field cooled (FC) curves and an exchange-bias effect for nanoparticles, a typical behavior of superparamagnetism.

The dependence of the particle's size on T_N in Co_3O_4 was reported by Mousavand *et al* [5]. In this research, an antiferromagnetic transition at $T_N = 32$ K for particles with ~92 nm diameter was presented. For particles with ~25 nm, a peak at $T_t = 10$ K was observed in χ_{dc} versus T curve, for $H \leqslant 25$ kOe [5]. The authors also observed an increase in the magnetization below T_N. This growth of magnetization and the transition at 10 K were attributed to spin-glass behavior related to the interaction between uncompensated moments in the crystal surface. On the other hand, in this paper the presence of the coercive field or remanent magnetization is not mentioned as expected for spin-glass systems.

In this paper, we contribute to the understanding of the nature of the second magnetic transition observed at 14 K, in addition to $T_N = 32$ K, already reported in the literature. The studies were performed in a polycrystalline sample.

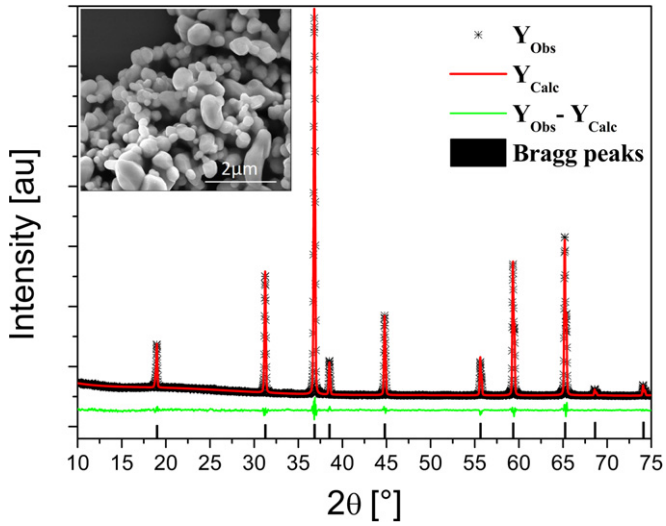

Figure 1. Room temperature XRD pattern for Co_3O_4 polycrystals. The black symbols (✳) indicate the observed data (Y_{Obs}), the red line refers to the calculated data (Y_{Calc}) using the Rietveld refinement method and the green line shows the difference between the observed and calculated data. Black bars correspond to the Bragg peaks of the Co_3O_4 pattern (ICSD Code: 24210).

2. Experimental

Co_3O_4 polycrystals were synthesized using the Pechini Method [15]. $CoSO_4{\cdot}7H_2O$ (P.A. Synth) was added to Ethylene Glycol (P.A. Mallinckrodt) and the solution was kept under constant stirring at 70 °C until the salt was completely dissolved. Afterwards, Citric Acid (P.A. Synth) was added to the solution. The resin obtained was then polymerized at 110 °C (1 h), and immediately after that it was burned in three steps, one at 300 °C (2 h), another at 500 °C (2 h) and finally at 800 °C (3 h). All the steps were carried out in a sealed crucible to inhibit the cobalt evaporation. The first two steps are useful to burn organic material and the last one is required to form the desired phase.

The microstructure of the Co_3O_4 was investigated using a field emission gun-scanning electron microscopy (FEG-SEM) and x-ray diffraction (XRD) with CuK_α radiation (1.54 Å). A 2θ scan was performed from 10° to 75° with 0.02° of increment. XDR data were analyzed using the Rietveld method [16, 17] in the GSAS/EXPGUI [18, 19] software, in order to exclude the presence of spurious phases and determine the phase lattice parameters.

Magnetic susceptibility as a function of the applied magnetic field, and magnetic susceptibility as a function of temperature in the range of 1.8–300 K, using ZFC (the field is applied after the sample cooling) and FC(the sample is cooled with an applied field) protocol were performed using a SQUID-VSM magnetometer (MPMS®3-Quantum Design). Ac magnetic susceptibility as a function of temperature for different driven frequencies (10 Hz, 100 Hz and 500 Hz), using $h_{ac} = 10$ Oe and $H_{dc} = 0$ Oe were also carried out.

3. Results and discussion

3.1. Structural and morphological properties

In order to determine the structural phases present in the sample and their lattice parameters, we performed a XRD measurement (figure 1). The Rietveld analysis exclusively revealed the presence of the cubic Co_3O_4 phase, belonging to the Fd-3m spatial group. The lattice parameters obtained for this phase were $a = b = c = 8.0869$ (1) Å, $\alpha = \beta = \gamma = 90°$, and are in agreement with the pattern used for comparison, ICSD Code: 24 210 ($a = b = c = 8.0835(6)$ Å).

Rietveld quality factors ($\chi^2 = 1.28$, $R_{wp} = 12.83\%$ and $RF^2 = 10.55\%$) showed conformity between experimental data and the fit curve, which can be confirmed by the good data fit and the small difference among Y_{Obs} (observed profile) and Y_{Cal} (calculated profile) shown in figure 1. FEG-SEM image (inset figure 1) shows particles with two predominant shapes, rounded and rounded-elongated, with diameters between 100 nm and 1200 nm. The crystallite size was estimated as being 68(4) nm on average by the well-known Scherrer equation [20].

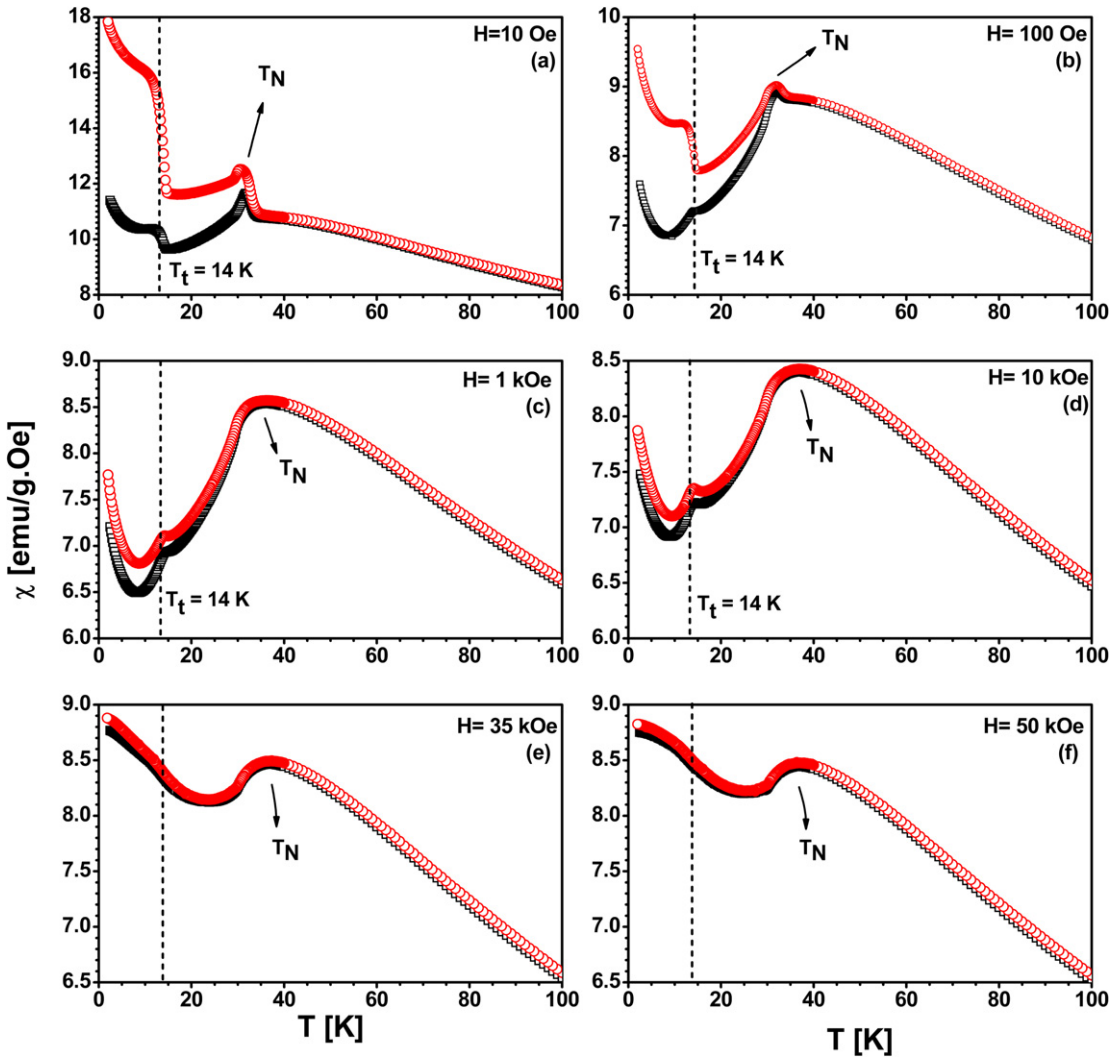

Figure 2. Dc magnetic susceptibility (χ_{dc}) as a function of temperature (T): (a) $H = 10$ Oe, (b) $H = 100$ Oe, (c) $H = 1$ kOe, (d) $H = 10$ kOe, (e) $H = 35$ kOe and (f) $H = 50$ kOe. Black squares and red circles indicate ZFC and FC measurements, respectively. T_N and T_t are also indicated by arrows.

3.2. Magnetic properties

In figure 2, we present dc magnetic susceptibility ($\chi_{dc} = M/H$) measurements as a function of temperature (T) for applied fields up to 50 kOe. Two phase transitions can be seen in the figure. The first one, $T_{N,}$ is the well described Néel temperature transition for Co_3O_4 bulk samples [5, 11] and originates from the interaction between Co^{2+} ions in the tetrahedral sites of the crystal. For our system, T_N is ~32 K as indicated by the maximum in χ_{dc} versus T curve for fields of 10 Oe (figure 2(a)) and 100 Oe (figure 2(b)). For $H \geqslant 1$ kOe T_N suffers a broadening.

The second transition was named T_t and is located at 14 K (figure 2). Below $T_{t,}$ ZFC and FC curves presented a large magnetic irreversibility for $H \leqslant 10$ kOe. Our results also showed that the T_t position is not dependent on the applied magnetic field despite the jump observed around T_t for $H = 10$ Oe (FC—figure 2(a)). For $H = 100$ Oe (figure 2(b)), this jump is still present in the FC curve while for $H = 1$ kOe (figure 2(c)) and 10 kOe (figure 2(d)) a sharp peak at T_t is present both in the ZFC and FC curves. However, for $H = 35$ kOe (figure 2(e)) and 50 kOe (figure 2(f)), the peak at T_t is almost suppressed, while the peak associated to T_N is still observed, which is expected behavior for a strong antiferromagnetic transition, as already reported for Co_3O_4 [5, 6, 11].

In order to investigate the nature of the transition observed at T_t, ac magnetic susceptibility as a function of the temperature measurements were performed in the temperature range of 2–60 K (figure 3(a)).

In χ'_{ac} as a function of temperature measurements (figure 3(a)), the peak at ~32 K is kept fixed by varying the frequency, in accordance with an antiferromagnetic transition characteristic of a bulk Co_3O_4 material. As can be seen in figure 3(a), the peak at T_t is also kept fixed with the frequency variation. This behavior is confirmed, both for T_f and T_N, by the derivative of χ' presented in figure 3(b). χ'' data for $f = 10$ Hz and 100 Hz

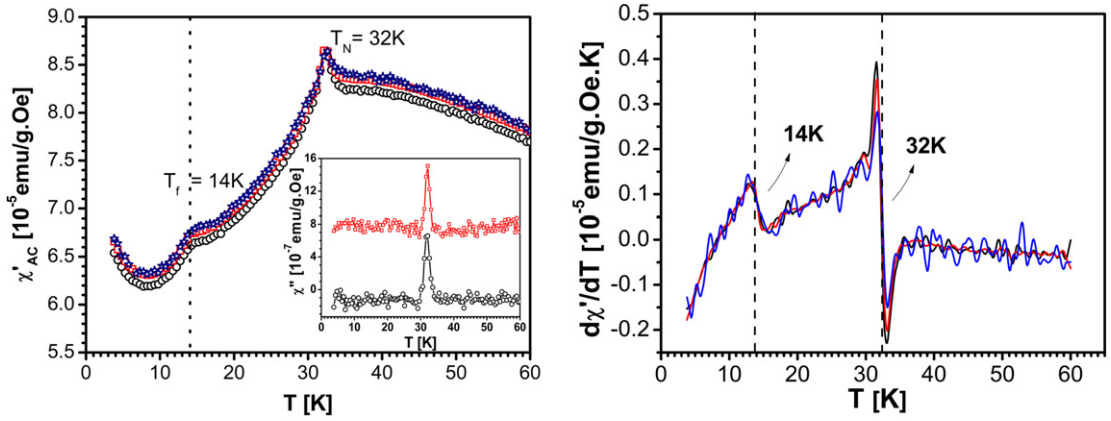

Figure 3. Ac magnetic susceptibility (χ') as a function of temperature (T) data for Co_3O_4 polycrystals. In (a) χ' component is presented. In the inset, the χ'' component is also showed. The values of χ'' for $f = 500$ Hz are not presented as they are below the limit of the equipment´s accuracy. In (b), the χ' derivative confirms that both the T_t and T_N peak positions are fixed for frequencies of 10 Hz (black curve), 100 Hz (red curve) and 500 Hz (blue curve).For these measurements $h_{ac} = 10$ Oe and $H_{dc} = 0$.

is presented in the inset of figure 3(a) where the peak associated to T_N is observed, while the peak associated to T_t is not visible as it is below the limit of the equipment´s accuracy. Previous studies published in the literature have associated a peak at temperatures below T_N in Co_3O_4 to spin-glass [9, 14] and superparamagnetic [7, 11, 14] behaviors. The characteristic of spin-glass like systems is the shift of the freezing temperature with the frequency variation and the applied magnetic field [10], an effect which was not observed in our measurements. In addition, for superparamagnetic systems a blocking temperature and coercive field below T_B are expected. In the present investigation, no shift of T_t with the variation of the driven frequency was observed and the absence of coercive field below T_N confirms that the peak observed in T_t is not associated with a metastable magnetic state.

In his ground-breaking work, Néel noted that antiferromagnetic materials in fine form particles could present superparamagnetism and ferromagnetism related to uncompensated spins in their sublattices [21–23]. For a bulk material, on the other hand, the effect of uncompensated spins can be neglected [24]. However, the number of uncompensated spins increased greatly as the particle size was reduced [24], the reduction in the particle size on a nanometric scale results in a high surface to volume ratio, finite-size effects and surface-interface effects, leading the system to an anomalous magnetic behavior different from that expected for the bulk phase [25, 26]. This effect was already reported for NiO [24, 26] and Co_3O_4 nanoparticles [27, 28]. Based on this research [24, 27, 28] as well as the results presented in figure 3, which show that the peak at T_t presents a behavior similar to that presented by T_N, i.e., does not change with the driven frequency variation, we propose that the transition at 14 K is also an antiferromagnetic transition. In this case, the transition at T_t is associated to the interaction between uncompensated moments in the surface of Co_3O_4 nanoparticles present in the sample, in other words, the transition at T_t is a grain size effect. The presence of different grain sizes gives rise to changes in the surface conditions leading to physical properties associated both to Co_3O_4 bulk and Co_3O_4 nanoparticles. The increase in magnetic susceptibility below T_t can be also attributed to uncompensated moments on the nanocrystals surface which are not completely canceled, as already observed for antiferromagnets by Mousavand *et al* [5] and Dutta *et al* [14].

The proposition presented above is also confirmed by M versus H measurements (figure 4). In figure 4, the failure to observe coercive field for temperatures below T_t preclude the behavior of spin-glass material [9].

Although magnetization as a function of applied magnetic field data shows an apparent linear behavior (figure 4), χ_{dc} (M/H) versus H data (figure 5) presented for different temperatures show that the system has two magnetic regimes, one around T_t and the other around T_N. Around T_t (figure 5(a)), a minimum at 4.5 kOe is observed. Above this field, χ_{dc} increases reaching a plateau at 55 kOe. This behavior shows that as the applied magnetic field is increased, a greater number of superficial magnetic moments are flipped tending to be aligned with the applied field. Our results show that for higher magnetic fields, the magnetic moments associated with the antiferromagnetic network on surface grains are no longer antiparallel, i.e., the antiferromagnetic phase is suppressed. This effect is expected because the interaction of these moments on the surface is weaker if compared to bulk antiferromagnetism. The anisotropy energy of the surface plays an important role in this symmetry breaking as the antiferromagnetic phase is suppressed to fields around 35 kOe, however the bulk antiferromagnetic phase transition is not affected by fields of the same intensity. As shown in figure 5(b), for temperatures around T_N, the magnetic susceptibility reaches a plateau for lower fields ($H < 500$ Oe) as expected

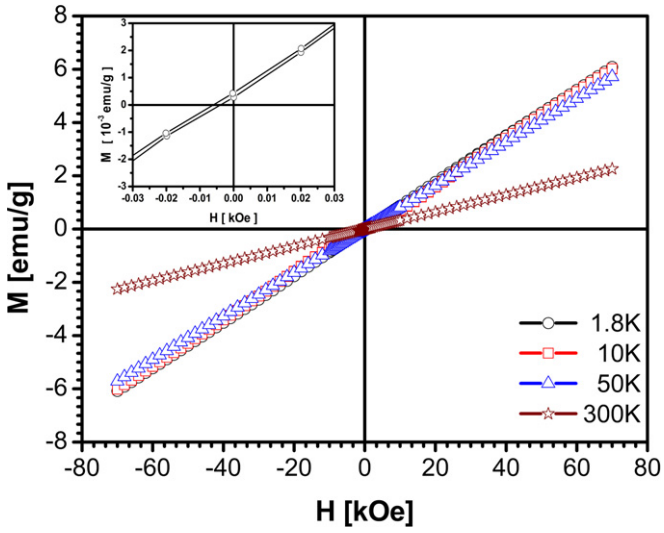

Figure 4. Magnetization (M) as a function of the applied magnetic field (H) for Co_3O_4 polycrystals between 1.8 and 300 K. The system does not present coercive field.

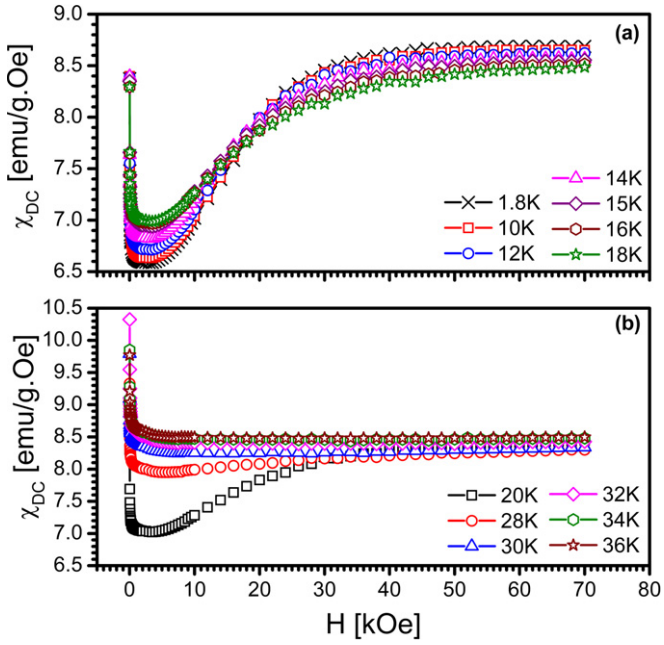

Figure 5. χ_{dc} as a function of the applied magnetic field (H) data from 0 to 70 kOe, for Co_3O_4 polycrystals. In (a) curves for 1.8 K, 10 K, 12 K, 14 K, 15 K, 16 K and 18 K are presented while in (b) we present the curves for 20 K, 28 K, 30 K, 32 K, 34 K and 36 K. The curves were obtained after cooling the samples to the desired temperature without magnetic field application, and after stabilizing the temperature, the field started to be charged.

for an antiferromagnetic material, i.e., the dependence of magnetization as a function of the applied magnetic field is linear.

4. Conclusions

In conclusion, Co_3O_4 polycrystals were produced using the Pechini Method with particle's sizes between 100 and 1200 nm and crystallite size of 68(4) nm. An antiferromagnetic transition at $T_N = 32$ K, expected and extensively reported in the literature for Co_3O_4, was observed further to a low temperature transition at $T_t = 14$ K which is suppressed for $H \geqslant 35$ kOe. An increase in the magnetic susceptibility in addition to

irreversibility between ZFC and FC data below T_t was also observed. The peak associated to T_N is still present even for field of 50 kOe as expected to a strong antiferromagnetic transition.

The non-observance of coercive field in the M versus H data for temperatures below T_t, added to the non peak shift at T_t in the χ' versus T data for different driven frequencies exclude the possibility of spin-glass or superparamagnetic behavior, unlike what was already observed in the Co_3O_4 nanoparticles. For our sample, T_t has the signature of an antiferromagnetic transition similar to that observed at T_N, although weaker. The transition at T_t is associated to interactions between superficial uncompensated moments present in the sample due to the particle size reduction. In other words, the observation of two antiferromagnetic transitions in the same sample is attributed to the broad particle size distribution, which leads the system to present the magnetic properties of both Co_3O_4 bulk and Co_3O_4 nanoparticles.

Acknowledgments

The authors would like to thank the financial support of FAPESP (09/54082-2, 2012/24025-0 and 2013/07296-2) and CNPq (500327/2014-9).

References

[1] Liu Y, Mi C, Su L and Zhang X 2008 Hydrotermal synthesis of Co_3O_4 microsphere as anode material for lithium-ion batteries *Electrochim. Acta* **53** 2507–13
[2] Kim H, Won Park D, Chul Woo H and Shik Chung J 1998 Reduction of SO_2 by CO to elemental sulfur over Co_3O_4–TiO_2 catalysts *Appl. Catal. B: Environ.* **19** 233–43
[3] Balouria V, Samanta S, Singh A, Debnath A K, Mahajan A, Bedi R K, Aswal D K and Gupta S K 2013 Chemiresistive gas sensing properties of nanocrystalline Co_3O_4 thin films *Sensors Actuators* B **176** 38–45
[4] Wang G, Shen X, Horvat J, Wang B, Liu H, Wexler D and Yao J 2009 Hydrothermal synthesis and optical, magnetic, and supercapacitance properties of nanoporous cobalt oxide nanorods *J. Phys. Chem.* C **113** 4357–61
[5] Mousavand T, Naka T, Sato K, Ohara S, Umetsu M, Takami S, Nakane T, Matsushita A and Adschiri T 2009 Crystal size and magnetic field effects in Co_3O_4 antiferromagnetic nanocrystals *Phys. Rev.* B **79** 1–5
[6] Hill A H, Harrison A, Ritter C, Yue W and Zhou W 2011 Neutron powder diffraction and magnetic studies of mesoporous Co_3O_4 *J. Magn. Magn. Mater.* **323** 226–31
[7] Zhu H T, Luo J, Liang J K, Rao G H, Li J B, Zhang J Y and Du Z M 2008 Synthesis and magnetic properties of antiferromagnetic Co_3O_4 nanoparticles *Physica B. Condens. Matter* **403** 3141–5
[8] Raveau B and Seikh M M 2012 Electronic and magnetic properties of cobaltites with 3D 'triangular lattice' *Cobalt Oxides: From Crystal Chemistry to Physics* (Weinheim: Wiley) ch 5 pp 211–47
[9] Hayakawa Y, Kohiki S, Sato M, Sonda Y, Babasaki T, Deguchi H, Hidaka A, Shimooka H and Takahashi S 2001 Magnetism of diluted Co_3O_4 nanocrystals *Physica E. Low-Dimens. Syst. Nanostruct.* **9** 250–2
[10] Mydosh J A 1993 *Spin Glasses An Experimental Introduction* (London: Taylor and Francis)
[11] Zhu H T, Luo J, Liang J K, Rao G H, Li J B, Zhang J Y and Du Z M 2008 Synthesis and magnetic properties of antiferromagnetic Co_3O_4 nanoparticles *Phys.* B (Amsterdam, Neth.) **403** 3141–5
[12] Ozkaya T, Baykal A, Toprak M S, Koseoglu Y and Durmuş Z 2009 Reflux synthesis of Co_3O_4 nanoparticles and its magnetic characterization *J. Magn. Magn. Mater.* **321** 2145–9
[13] Takada S, Fujii M and Kohiki S 2001 Intraparticle magnetic properties of Co_3O_4 Nanocrystals *Nano Lett.* **1** 379–82
[14] Dutta P, Seehra M S, Thota S and Kumar J 2008 A comparative study of the magnetic properties of bulk and nanocrystalline Co_3O_4 *J. Phys.: Condens. Matter* **20** 015218
[15] Pechini M P 1967 *USA Patent No* 3.330.697
[16] Young R A 1993 *The Rietveld Method* (New York: Oxford Univ. Press)
[17] Rietveld H M 1969 A profile refinement method for nuclear and magnetic structures *J. Appl. Crystallogr.* **2** 65–71
[18] Larson A C and Von Dreele R B 2004 General structure analysis system (GSAS) *Los Alamos National Laboratory Report* 86-748
[19] Toby B H 2001 EXPGUI, a graphical user interface for GSAS *J. Appl. Crystallogr.* **34** 210–3
[20] Scherrer P 1918 Bestimmung der Größe und der inneren Struktur von Kolloidteilchen mittels Röntgenstrahlen *Göttinger Nachrichten Gesell.* **1918** 98–100
[21] Néel L 1961 *C. R. Acad. Sci., Paris* **252** 4075
[22] Néel L 1961 *C. R. Acad. Sci., Paris* **153** 9
[23] Néel L 1961 *C. R. Acad. Sci., Paris* **253** 203
[24] Schuele W J and Deetscreek V D 1962 Appearance of a weak ferromagnetism in fine particles of antiferromagnetic materials *J. Appl. Phys.* **33** 1136–7
[25] Verma V and Katiyar M 2015 Origin of intrinsic ferromagnetism in undoped antiferromagnetic NiO thin films *J. Phys. D. Appl. Phys.* **48** 235003
[26] Richardson J T, Yiagas D I, Turk B, Forster K and Twigg M V 1991 Origin of superparamagnetism in nickel oxide *J. Appl. Phys.* **70** 6977–82
[27] Tomou A, Gournis D, Panagiotopoulos I, Huang Y, Hadjipanayis G C and Kooi B J 2006 Weak ferromagnetism and exchange biasing in cobalt oxide nanoparticle systems *J. Appl. Phys.* **99** 1–6
[28] Bisht V and Rajeev K P 2011 Non-equilibrium effects in the magnetic behavior of Co_3O_4 nanoparticles *Solid State Commun.* **151** 1275–9